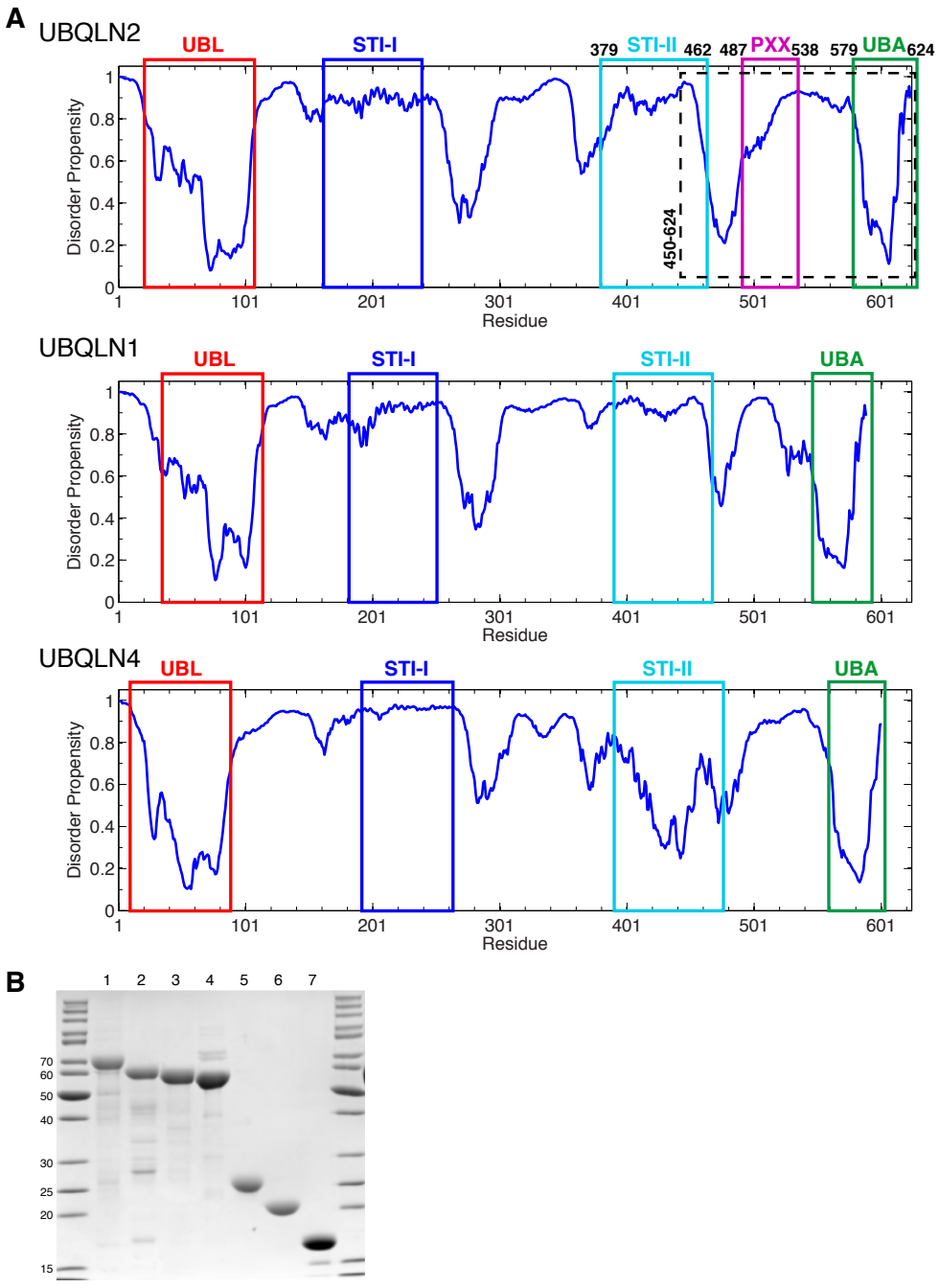

Figure S1, related to Figure 2. Sequence-based order/disorder predictions of UBQLNs and SDS-PAGE gel of purified UBQLN2 constructs. (A) Domain architecture of UBQLNs are noted in solid boxes. Disorder propensity was calculated using PONDR-FIT (Xue et al., 2010). Disorder propensity plot for UBQLN2 identifies part of STI1-II as being ordered, and guides the design of the UBQLN2 450-624 construct (dotted lines). (B) Samples on SDS-PAGE gel are loaded as: 1: Full-length UBQLN2, 2: UBQLN2 ΔUBA, 3: UBQLN2 ΔPXX, 4: UBQLN2 Δ379-486, 5: UBQLN2 379-624, 6: UBQLN2 450-624, 7: UBQLN2 487-624. Molecular weight markers are labeled on left side in kDa.

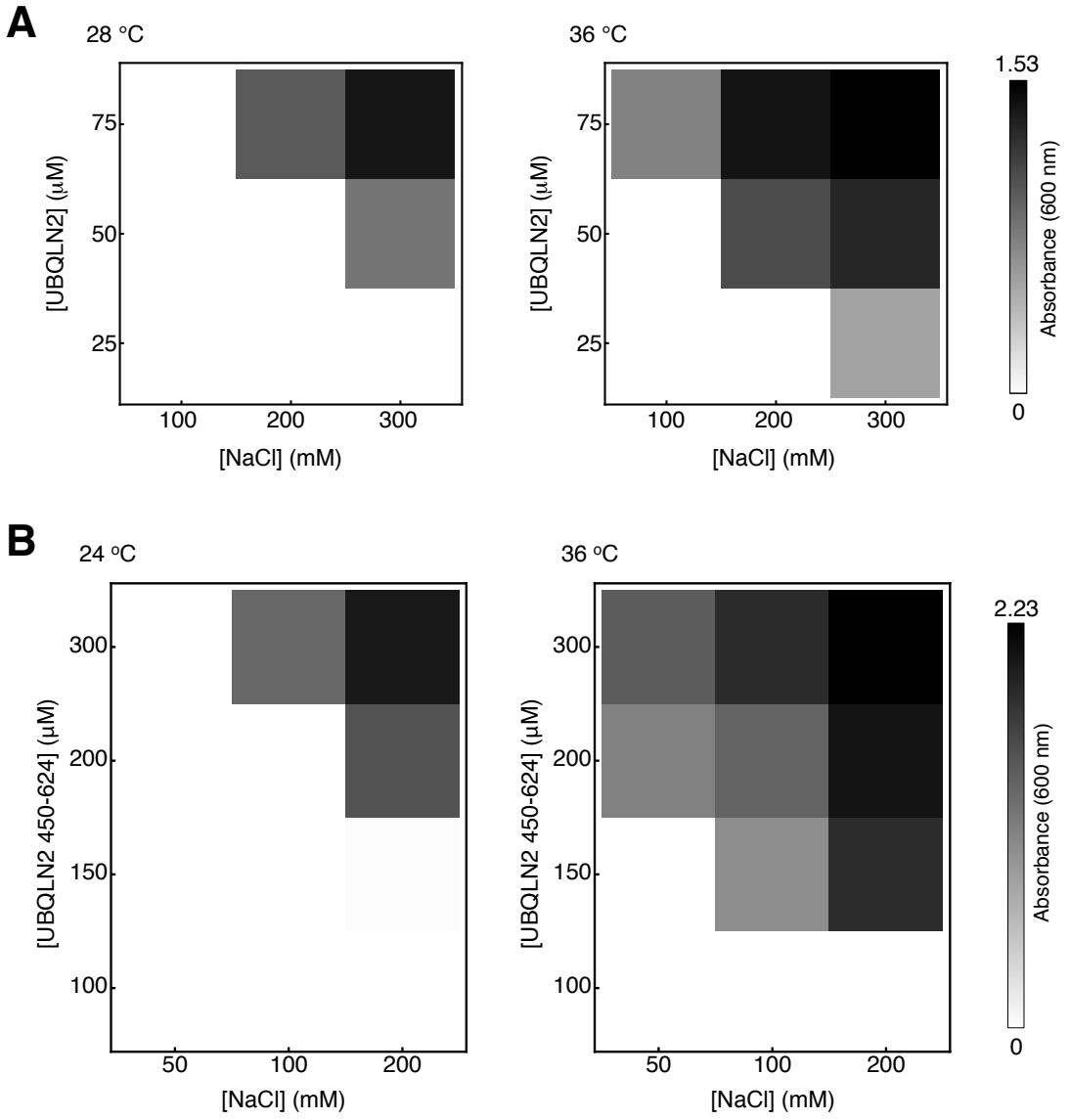

Figure S2, related to Figures 1 and 2. Phase diagrams for full-length UBQLN2 and UBQLN2 450-624. Results are shown from spectrophotometric assays of (A) full-length UBQLN2 at 28°C and 36°C, and (B) UBQLN2 450-624 at 24°C and 36°C. Note that phase separation is induced at higher protein and higher NaCl concentrations, as observed with all UBQLN2 constructs that phase separate.

A

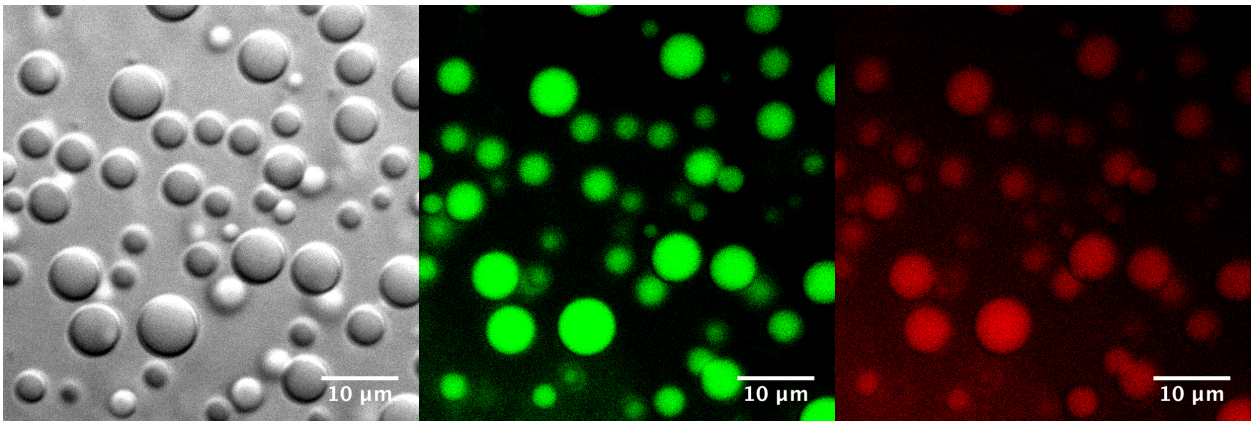
10 µm
10 µm
10 µm

B

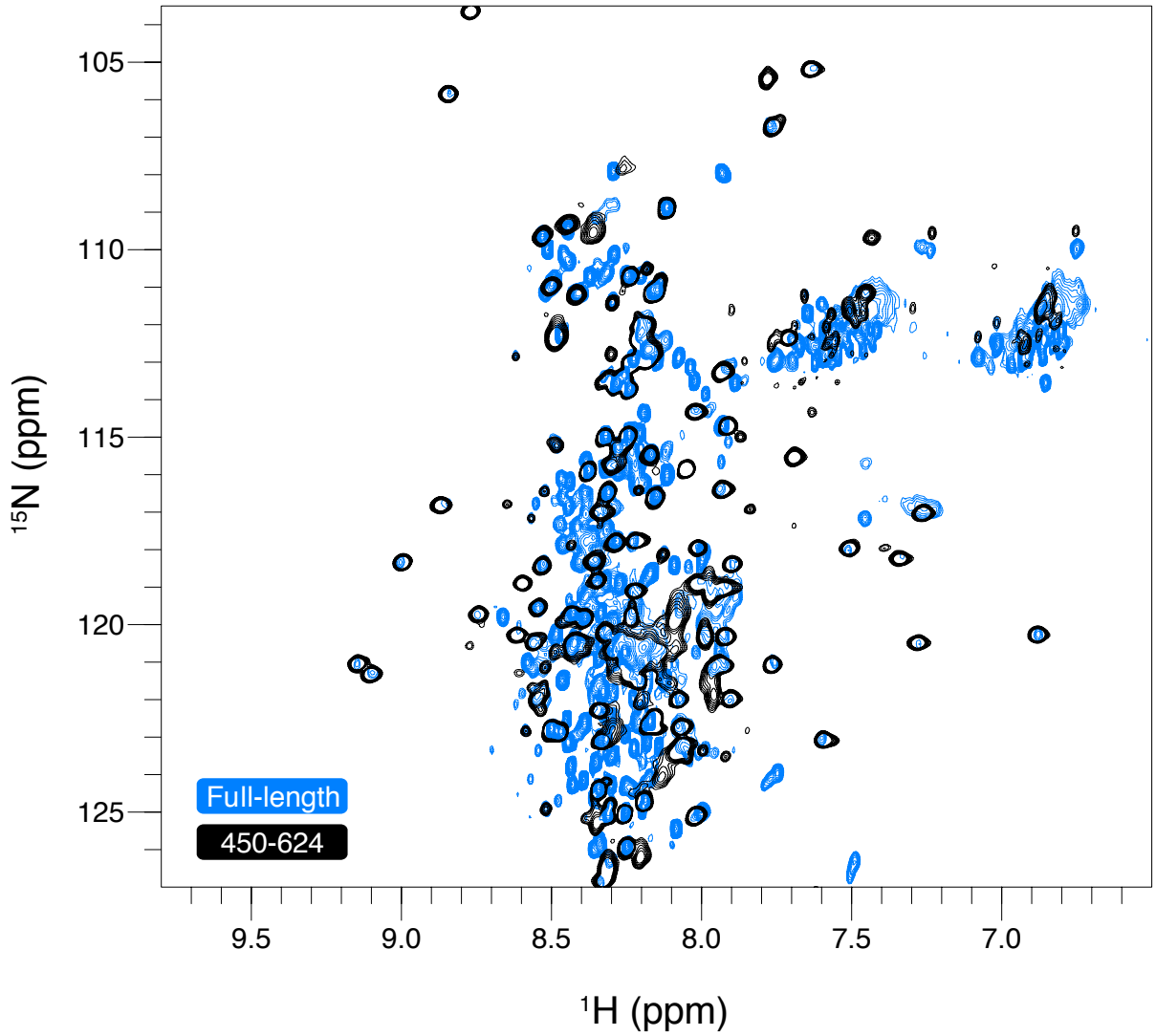
105
110
115
120
125
^{15}N (ppm)
9.5
9.0
8.5
8.0
7.5
7.0
^{1}H (ppm)
Full-length
450-624

Figure S3, related to Figures 2 and 3. UBQLN2 450-624 construct exhibit similar properties to full-length UBQLN2. (A) UBQLN2 450-624 colocalizes with full-length UBQLN2 into same droplets. DIC microscopy (left) shows LLPS of UBQLN2 450-624 and full-length UBQLN2 mixed in equimolar amounts (50 μM) at pH 6.8 200 mM NaCl. Full-length UBQLN2 was fluorescently-tagged with DyLight-488 (middle) and UBQLN2 450-624 was fluorescently-tagged with DyLight-650 (right). (B) ^{1}H-^{15}N NMR spectral overlay of UBQLN2 450-624 (black contours) with full-length UBQLN2 (sky blue contours). Many UBQLN2 450-624 resonances overlap with those in full-length UBQLN2, indicating that the chemical microenvironment of these residues are similar in both proteins. Contour settings for UBQLN2 450-624 spectra were adjusted to highlight peak outlines.

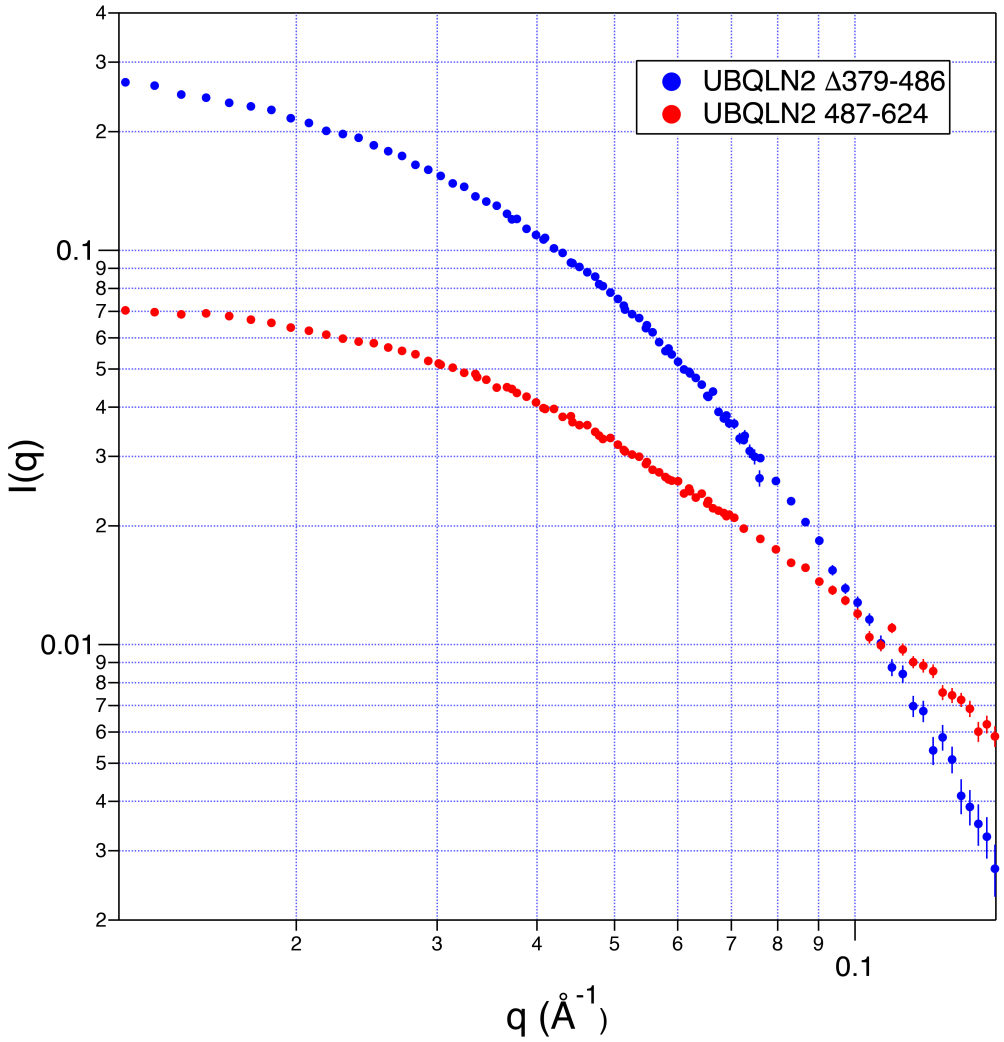

Figure S4, related to Figure 2. Small angle neutron scattering (SANS) curves for UBQLN2 constructs, obtained at the NIST Center for Neutron Research. SANS measurements confirmed that UBQLN2 Δ379-486 and UBQLN2 487-624 constructs were monomeric, as observed forward scattering I(0) measurements were within 10% of expected monomeric I(0) values (Table S1).

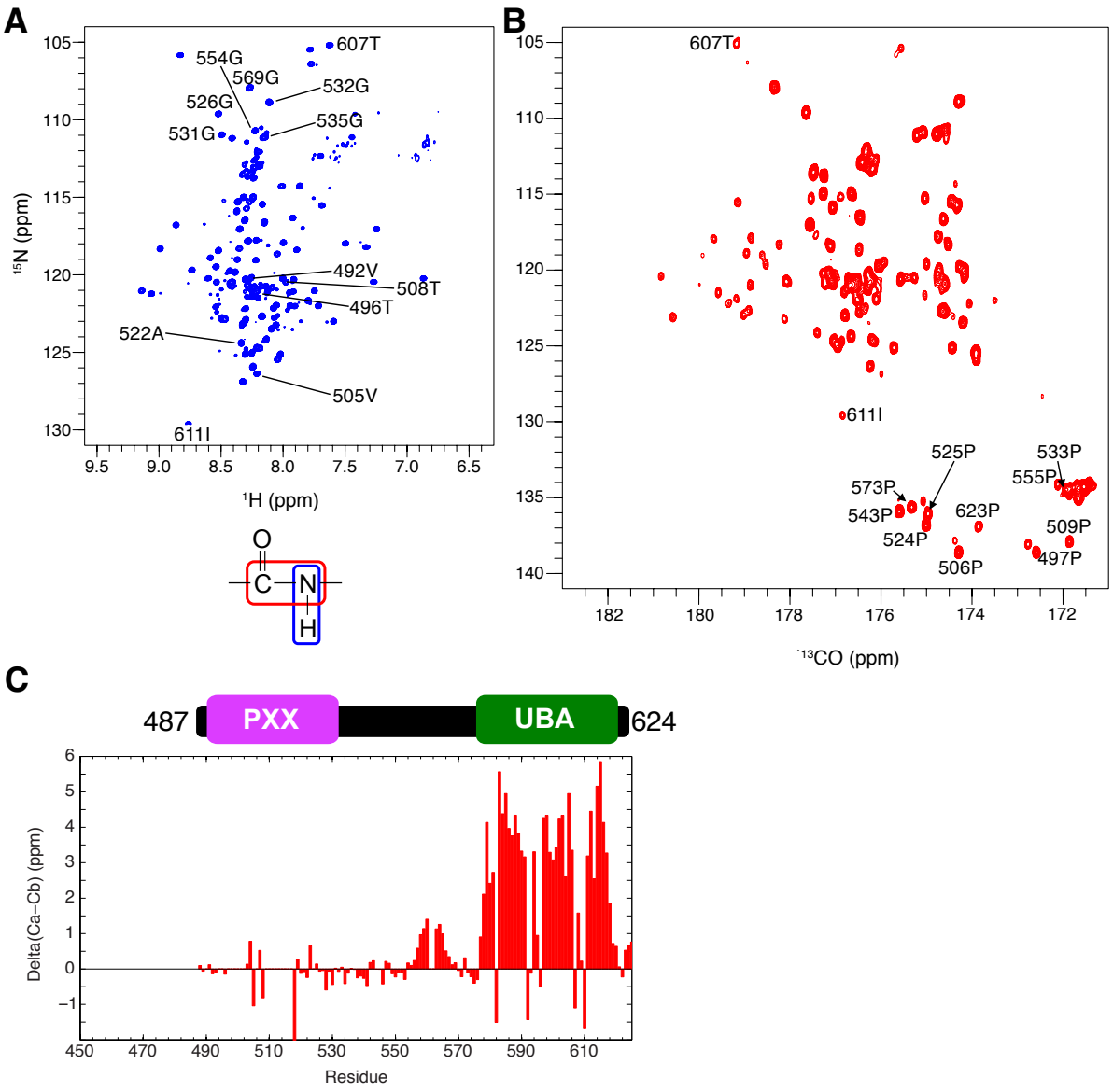

Figure S5, related to Figure 3. NMR analysis of UBQLN2 487-624. (A) ^{1}H-^{15}N TROSY-HSQC spectra and (B) ^{15}N-^{13}C (HACA)CON spectra with highlighted residues showing resonance assignments for residues in the proline-rich region (Pxx) and select assignments of the UBA domain. (C) Residue-by-residue secondary structure plot highlighting helical propensity between residues 550 and 570, and helical segments in the globular UBA domain. Spectra were collected at 25^{o}C using 400 μM protein, in pH 6.8 buffer with no added NaCl.

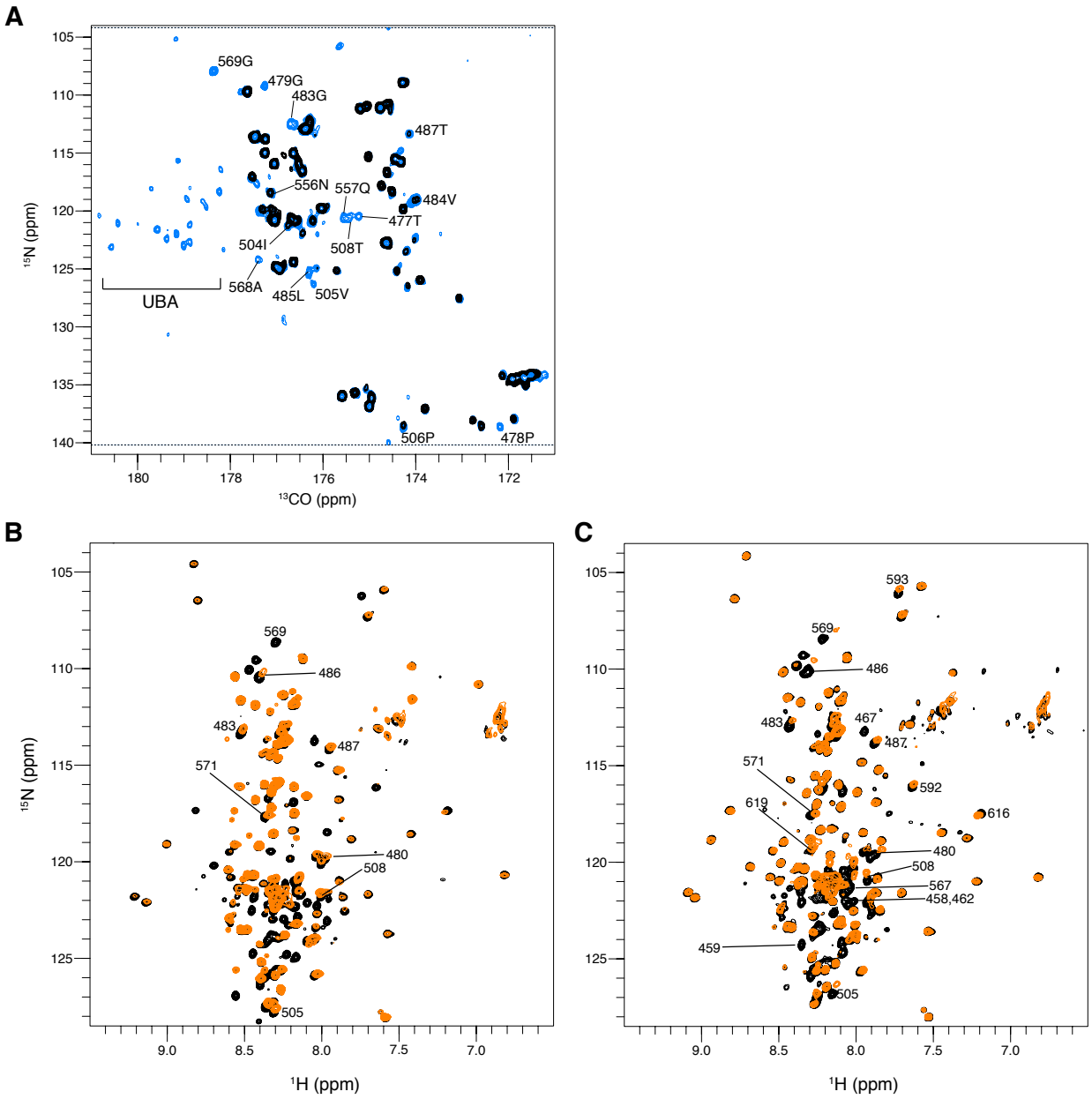

Figure S6, related to Figure 4. UBQLN2 450-624 and UBQLN2 379-624 constructs exhibit concentration-dependent chemical shifts. (A) ^{15}N-^{13}CO (HACA)CON NMR spectra of UBQLN2 450-624 at 25^{o}C at two protein concentrations: 50 μM (skyblue) and 200 μM (black). Marked residues are those that are attenuated at higher protein concentrations. Many of these attenuations include residues 470-490, 504-508, and 556-569. Contours are set to the same level for both protein concentrations. Note that the 50 μM experiment was collected with 96 scans rather than 32 scans for the 200 μM experiment. (B,C) Overlay of UBQLN2 379-624 (orange) and 450-624 (black) NMR spectra. (B) ^{1}H-^{15}N TROSY-HSQC overlay of 200 μM protein at 10^{o}C. (C) ^{1}H-^{15}N TROSY-HSQC overlay of 50 μM protein at 25^{o}C. All spectra were collected under identical conditions (e.g. same number of scans, receiver gain, and number of indirect

dimension points). Contours for spectra of 379-624 in B were lowered to see UBA peaks, but contours are identical for both proteins in C. Note that many resonances belonging to residues 450-480 in UBQLN2 379-624 were broadened beyond detection, and chemical shift perturbations were observed for residues 480-487, 505-508, 567-571, 592-593, 616-619 (labeled residues on spectra). All spectra were collected in pH 6.8 buffer containing 20 mM NaPhosphate under conditions where proteins were not phase-separated.

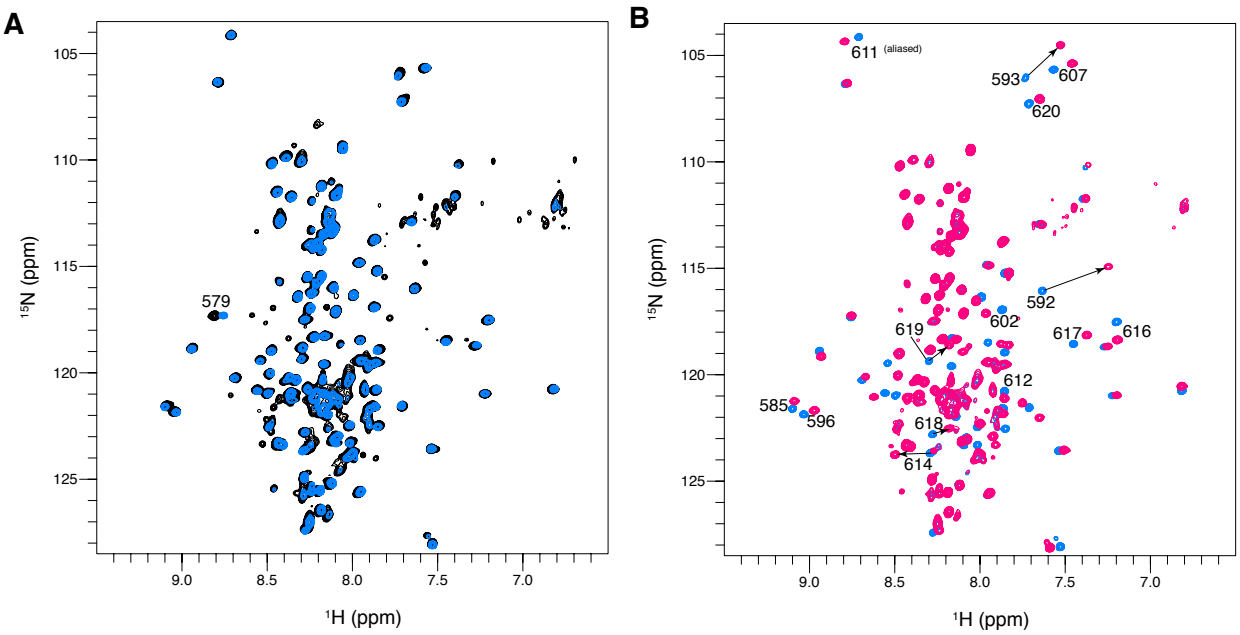

Figure S7, related to Figure 6. NMR analysis of UBQLN2 450-624 phase separation. (A) ^{1}H-^{15}N TROSY-HSQC overlay of 200 µM UBQLN2 450-624 in the absence of NaCl (black) and in the presence of 200 mM NaCl (skyblue) at 25^{o}C (induced phase separation). Note the absence of chemical shift changes, but overall reduction in peak intensity. (B) ^{1}H-^{15}N TROSY-HSQC overlay of 200 µM UBQLN2 450-624 in the absence of Ub (skyblue) and presence of 400 µM Ub (magenta). Spectra were collected using pH 6.8 buffer with 200 mM NaCl. Chemical shift perturbations are observed only for residues in the UBA domain. All experiments were collected and processed under identical NMR conditions, and contour settings were set to the same level for all spectra.

Table S1. SANS parameters for UBQLN2 Δ379-486 and UBQLN2 487-624 constructs, related to Figure S4.

	Expected I(0) [a] (cm^{-1})	Observed I(0) [b] (cm^{-1})	$R_g \times q_{min}$ [c]	$R_g \times q_{max}$ [c]	R_g (Å) [d]
UBQLN2 Δ379-486 (5 mg/mL) [e]	0.265	0.290 ± 0.002	0.569	1.311	46.5 ± 0.4
UBQLN2 487-624 (4.5 mg/mL) [e]	0.068	0.075 ± 0.001	0.533	1.232	34.6 ± 0.4

[a] Expected I(0) values determined using small angle scattering calculator (Sarachan et al., 2013).
[b] I(0) and standard errors were determined from the linear fit of $\ln(I(q))$ vs. q^2.
[c] Data range chosen for Guinier fit.
[d] Radius of gyration (R_g) and standard errors were determined from the linear fit of $\ln(I(q))$ vs. q^2.
[e] SANS measurements were obtained in pH 6.8 buffer with no added NaCl, at 25°C.

Table S2. Diffusion tensor characteristics of the UBA domain in UBQLN2 constructs, related to Figure 4.

	Diffusion tensor								
Protein [a]	D_{xx} [b]	D_{yy} [b]	D_{zz} [b]	α [c]	β [c]	γ [c]	τ_c [d]	Anisotropy [e]	Rhombicity [f]
487-624	1.98 (0.19)	2.39 (0.28)	3.93 (0.53)	3 (8)	88 (8)	101 (33)	6.01 (0.45)	1.79 (0.28)	0.36 (0.07)
450-624	1.51 (0.14)	1.83 (0.19)	2.53 (0.20)	179 (10)	94 (13)	83 (34)	8.52 (0.45)	1.52 (0.16)	0.54 (0.10)

[a] NMR ^{15}N relaxation measurements were collected using 200 µM protein in pH 6.8 buffer containing 20 mM NaPhosphate in the absence of added NaCl.
[b] Principal values of the rotational diffusion tensor (D_{xx}, D_{yy}, D_{zz}, in 10^7 s^{-1}), ordered as $D_{zz} \geq D_{yy} \geq D_{xx}$.
[c] Euler angles (α, β, γ in degrees) according to the y-convention characterize orientation of the principal axes frame of the alignment or diffusion tensor with respect to the coordinate frame of UBA (PDB 2JY6). α,β,γ are chosen such that all values fall between 0° and 180°.
[d] Overall rotational correlation time, $\tau_c = 0.5\left(D_{xx} + D_{yy} + D_{zz}\right)^{-1}$, in nanoseconds.
[e] Anisotropy of the diffusion tensor calculated as $\xi = 2D_{zz}/\left(D_{xx} + D_{yy}\right)$.
[f] Rhombicity of the diffusion tensor calculated as $\eta = 1.5\left(D_{yy} - D_{xx}\right)/\left[D_{zz} - 0.5\left(D_{xx} + D_{yy}\right)\right]$.